Redox Biology 13 (2017) 266–277

Contents lists available at ScienceDirect

Redox Biology

journal homepage: www.elsevier.com/locate/redox

Research Paper

HPW-RX40 prevents human platelet activation by attenuating cell surface protein disulfide isomerases

Po-Hsiung Kung[a], Pei-Wen Hsieh[b,e], Ying-Ting Lin[c], Jia-Hau Lee[c], I-Hua Chen[a], Chin-Chung Wu[a,d,*]

[a] Graduate Institute of Natural Products, Kaohsiung Medical University, Kaohsiung, Taiwan
[b] Graduate Institute of Natural Products, School of Traditional Chinese Medicine, College of Medicine, Chang Gung University, Taoyuan, Taiwan
[c] Department of Biotechnology, Kaohsiung Medical University, Kaohsiung, Taiwan
[d] Department of Marine Biotechnology and Resources, National Sun Yat-sen University, Kaohsiung, Taiwan
[e] Department of Anesthesiology, Chang Gung Memorial Hospital, Taoyuan, Taiwan

ARTICLE INFO

Keywords:
HPW-RX40
Nitrostyrene
Protein disulfide isomerase
Platelets
Anti-thrombotic agents

ABSTRACT

Protein disulfide isomerase (PDI) present at platelet surfaces has been considered to play an important role in the conformational change and activation of the integrin glycoprotein IIb/IIIa (GPIIb/IIIa) and thus enhances platelet aggregation. Growing evidences indicated that platelet surface PDI may serve as a potential target for developing of a new class of antithrombotic agents. In the present study, we investigated the effects of HPW-RX40, a chemical derivative of β-nitrostyrene, on platelet activation and PDI activity. HPW-RX40 inhibited platelet aggregation, GPIIb/IIIa activation, and P-selectin expression in human platelets. Moreover, HPW-RX40 reduced thrombus formation in human whole blood under flow conditions, and protects mice from $FeCl_3$-induced carotid artery occlusion. HPW-RX40 inhibited the activity of recombinant PDI family proteins (PDI, ERp57, and ERp5) as well as suppressed cell surface PDI activity of platelets in a reversible manner. Exogenous addition of PDI attenuated the inhibitory effect of HPW-RX40 on GPIIb/IIIa activation. Structure-based molecular docking simulations indicated that HPW-RX40 binds to the active site of PDI by forming hydrogen bonds. In addition, HPW-RX40 neither affected the cell viability nor induced endoplasmic reticulum stress in human cancer A549 and MDA-MB-231 cells. Taken together, our results suggest that HPW-RX40 is a reversible and non-cytotoxic PDI inhibitor with antiplatelet effects, and it may have a potential for development of novel antithrombotic agents.

1. Introduction

Protein disulfide isomerase (PDI) is an enzyme ubiquitously expressed in various cells. The enzyme catalysts the reduction, oxidation, and isomerization of disulfide bonds, and takes part in many physiological functions, such as protein folding and chaperone activity in endoplasmic reticulum (ER) [1,2]. In addition, PDI has also been found on the membrane surfaces of several kinds of cells, including platelets, vascular endothelial cells, and neutrophils [3]. Currently, there are more than 20 PDI family members known in humans. Among them, PDI is the prototypic member and has been studied more extensively than other members [4]. A number of evidences indicated that the reductase activity of platelet surface PDI contributes to the activation of glycoprotein (GP) IIb/IIIa (integrin $\alpha_{IIb}\beta_3$) which is the major receptor on the platelet surface responsible for platelet adhesion and aggregation [5,6].

Upon platelet stimulation by agonists, such as thrombin, collagen, ADP, and thromboxane A_2 (TxA_2), PDI on the surface of platelets reduces or rearranges disulfide bonds within GPIIb/IIIa, thus enhances the conformational change of GPIIb/IIIa induced by intracellular stimulatory signals (so called “inside-out” signaling) that results in a high-affinity state for fibrinogen binding [7,8]. The ligation of GPIIb/IIIa and fibrinogen leads to platelet aggregation and further trigger a second wave of intracellular stimulatory signals (so called “outside-in” signaling) that results in stabilization of platelet aggregates, platelet

Abbreviations: CHOP, CCAAT-enhancer-binding protein homologous protein; Di-E-GSSG, dieosin glutathione disulfide; $DiOC_6(3)$, 3,3′-dihexyloxacarbocyanine iodide; DTT, dithiothreitol; GSSG, oxidized glutathione; ER, endoplasmic reticulum; EGSH, eosin-coupled glutathione; ERp5, endoplasmic reticulum protein 5; ERp57, endoplasmic reticulum protein 57; ERp72, endoplasmic reticulum protein 72; GPIIb/IIIa, glycoprotein IIb/IIIa; GRP78, 78 kDa glucose-regulated protein; MNS, 3,4-methylenedioxy-nitrostyrene; PAO, phenylarsine oxide; PBS, phosphate buffered saline; PDI, protein disulfide isomerase; SDS-PAGE, polyacrylamide gel electrophoresis; TG, Thapsigargin; TMX, transmembrane thioredoxin-related protein; U46619, 9,11-dideoxy-9,11-methanoepoxy PGF2α

* Corresponding author at: Graduate Institute of Natural Products, Kaohsiung Medical University, Kaohsiung, Taiwan.
E-mail address: ccwu@kmu.edu.tw (C.-C. Wu).

http://dx.doi.org/10.1016/j.redox.2017.05.019
Received 3 April 2017; Received in revised form 22 May 2017; Accepted 25 May 2017
Available online 29 May 2017

spreading, and clot retraction [9]. PDI is considered to be involved in maintaining of the ligation of GPIIb/IIIa and fibrinogen, and thus also contributes "outside-in" signaling [10,11].

The physiological relevance of PDI has been validated by using specifically blocking antibodies and genetic methodologies. The PDI antibody RL90 has been shown to inhibit GPIIb/IIIa activation and platelet aggregation. Infusion of RL90 inhibited platelet thrombus formation and fibrin generation in a murine model [12]. In platelet-specific PDI-deficient mice, platelet accumulation in the injury sites of blood vessels was reduced [13]. Of note, tail bleeding time in platelet-specific PDI-deficient mice were not significantly increased, this finding implies that PDI inhibition may have less risk of bleeding complications. Therefore, the platelet surface PDI may serve as a potential target for developing of a new class of antithrombotic agents.

In our previous studies, a series of nitrostyrene derivatives have been evaluated for their antiplatelet effects. 3,4-methylenedioxy-β-nitrostyrene (MNS) is the prototype compound, it prevented platelet aggregation and activation through inhibition of tyrosine kinases src and syk [14–16]. Further structural modification of MNS led to discovery of a more potent antiplatelet compound, HPW-RX40 [17]. Interesting, HPW-RX40 did not inhibit platelet tyrosine kinases; this led to suggest that other mechanisms were involved in its actions. Because MNS also exhibited PDI-inhibiting activity in human breast cancer cells [18], we wondered if PDI inhibition is an underlying mechanism for HPW-RX40's antiplatelet effects. In the present study, our results indicated that HPW-RX40 is a potent PDI inhibitor with antithrombotic activity; moreover, its mode of action on PDI is distinct from the putative PDI inhibitors rutin and phenylarsine oxide.

2. Materials and methods

2.1. Materials

HPW-RX40 (2-Methoxy-4-[(E)-2-nitrovinyl]phenyl 2,3-dichlorobenzoate) was synthesized according the methods described previously [17]. Bovine α-thrombin was purchased from Biovision, (Mountain View, CA, USA). Collagen (Type I, equine tendon) was from Helena Laboratories (Beaumont, TX, USA). Fibrinogen, U46619 (9,11-dideoxy-9,11-methanoepoxy PGF2α), 12-O-tetradecanoylphorbol-13-acetate (TPA), A23187, eosin isothiocyanate, oxidized glutathione (GSSG), and phenyl arsenoxide (PAO) were from Sigma-Aldrich (St. Louis, MO, USA). Alexa Flour 488-conjugated phalloidin, was obtained from Molecular Probes (Eugene, OR, USA). Thapsigargin and rutin were purchased from Cayman Chemical (Ann Arbor, MI, USA). Human recombinant PDI, ERp72, and Fura-2/AM were purchased from Enzo Life Sciences (Farmingdale, NY, USA); Human recombinant ERp57 and anti-P47 Ab were from Abcam (Cambridge, UK), and ERp5 was from Pro-Spec Protein Specialists (Rehovot, Israel). Anti-PDI Ab was from Pierce/Thermo (Rockford, IL, USA); anti-GRP78 Ab was from Genetex (Irvine, CA, USA); phospho-PKC substrate antibody and anti-CHOP Ab were from Cell Signaling Technology (Beverly, MA, USA); anti-actin was from Santa Cruz Biotechnology (Santa Cruz, CA, USA). All other chemicals were purchased from Sigma Chemical Co.

2.2. Preparation of washed human platelets

Human blood anticoagulated with acid citrate dextrose (ACD) was obtained from healthy human volunteers who had not taken any drugs or supplements in the last two weeks. This study was approved by the Institutional Review Board of Kaohsiung Medical University, and informed consent was acquired from all volunteers. The platelet suspension was prepared according to the experimental procedures described previously [19]. The final concentration of platelets was adjusted to 3×10^8 mL^{-1} in Tyrode's solution (2 mM Ca^{2+}, 1 mM Mg^{2+} 11.1 mM glucose, 0.35% (w/v) bovine serum albumin, 5.6 mM glucose).

2.3. Measurement of platelet aggregation

Platelet aggregation was measured by using turbidimetric aggregometer (Chrono-Log Co., USA) under stirring conditions (1200 rpm) at 37 °C. The extent of platelet aggregation was measured as the maximal increase of light transmission after the addition of stimulators.

2.4. Measurement of GPIIb/IIIa activation and P-selectin expression by flow cytometry

Flow cytometric analysis of GPIIb/IIIa activation and P-selectin expression was conducted by using FITC-conjugated PAC-1 and P-selectin monoclonal antibody, respectively [20]. In order to prevent the formation of platelet aggregates, low concentrations of washed human platelets (3×10^7 platelets mL^{-1}) and non-stirring conditions were used. Platelets were pre-incubated with DMSO or HPW-RX40 for 3 min, and then stimulated with thrombin in the presence of excessive amounts of FITC-conjugated PAC-1 or P-selectin monoclonal antibody for 15 min at room temperature. The samples were fixed with 1% (w/v) paraformaldehyde and analyzed with a BD Accuri C6 flow cytometer (Becton Dickinson). Platelets were identified by signal amplification for forward and side scatter. The levels of PAC-1 binding and P-selectin expression were expressed as the percentages of positive cells.

2.5. In vitro thrombus formation assay

The experiments were applied according to the instruction of the manufacturer, with slightly modification. Flow chambers (μ-Slide VI 0.1, ibidi GmbH, Munich, Germany) was coated with Type I collagen from calf skin (Sigma-Aldrich, St. Louis) at a concentration 500 μg mL^{-1} in the flow chambers for 1 h at 37 °C. Citrated whole blood was incubated with $DiOC_6(3)$ 2 μM for 10 min at 37 °C in the absence or presence of HPW-RX40, and labeled blood was perfused through the flow chamber by syringe pump (KD Scientific Inc., New Hope, PA) for 2 min at a wall shear rate of 1500 S^{-1} (15 dyn cm$^{2-1}$). The channels were then washed with PBS buffer for 2 min at the same shear rate to remove non-adherent cells. The Images of adherent platelets were recorded with a CCD camera and the adherent area of platelets was analyzed by using ImageJ software (National Institutes of Health, Bethesda, MD) [21].

2.6. $FeCl_3$-induced carotid artery thrombus formation in mice

All animals used in this study were approved by the IACUC of the Kaohsiung Medical University. Male mice weighing 20–25 g (C57BL/6 age 6–8 weeks) were anesthetized using urethane (50 mg kg^{-1}) by intraperitoneal injection. Carotid artery thrombosis was induced according to the method described [22] with some modifications. The right carotid artery was exposed by blunt dissection, and a 2 × 4 mm filter paper soaked in 10% (w/v) $FeCl_3$ was applied to the artery for 3 min. After removing the filter paper, pulsed-wave Doppler analysis was carried out using a VEVO 2100 System with a small animal transducer (18–38 MHz) and the VEVO Imaging Station (Visualsonics) [23]. The occlusion time was determined when the blood flow completely stopped for at least 1 min, and the humane endpoint was 30 min after removal of $FeCl_3$ filter paper no matter whether the artery was occlusive.

2.7. Measurement of intracellular Ca^{2+} mobilization

Intracellular Ca^{2+} mobilization of platelets was measured by the method described previously [24]. In brief, platelets were incubated with fura-2/AM (2.5 μM) at 37 °C for 30 min. After washing twice, the fura-2-loaded platelets were finally suspended in Ca^{2+}-free Tyrode's solution at a concentration of 5×10^7 platelets mL^{-1}. Calcium (1 mM)

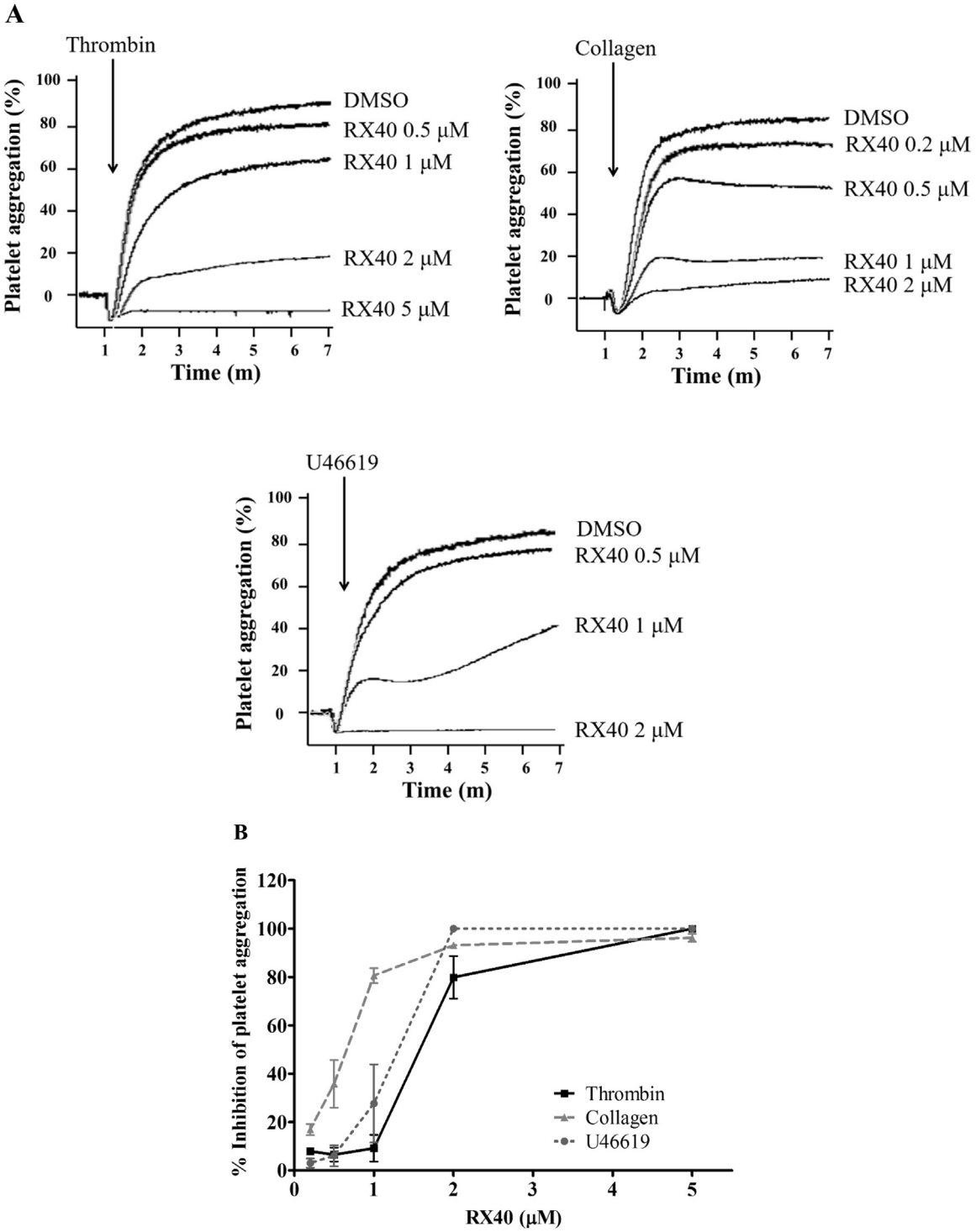

Fig. 1. HPW-RX40 inhibits platelet aggregation induced by various agonists. (A) Washed human platelets were incubated with DMSO (vehicle control) or HPW-RX40 (RX40) at 37 °C for 3 min, then thrombin (0.05 U mL^{-1}), collagen (5 μg mL^{-1}) or U46619 (2 μM) was added to trigger platelet aggregation. Tracings are representatives of three independent experiments. (B) Percentages of inhibition of platelet aggregation are presented as mean ± SEM. (n = 3).

was added to the fura-2-loaded platelets 1 min before stimulation with thrombin. Fluorescence (Ex 339 nm, Em 500 nm) was measured with a fluorescence spectrophotometer (Model F4000; Hitachi, Tokyo, Japan).

2.8. Fibrinogen cell adhesion assay

Adhesion assay described previously with some modification was used [25]. Coverslips were placed in the 24-well plate and coated with fibrinogen at a concentration 50 μg mL^{-1} overnight at 4 °C. After blocking with 1% (w/v) BSA for 2 h, 1 × 10^7 platelets mL^{-1} treated with HPW-RX40 were added to the plate and incubated at room temperature for another 1 h, and non-adherent platelets were removed with PBS. The coverslips were fixed with 2% (w/v) paraformaldehyde in PBS, permeabilized with 0.05% (w/v) Triton X-100 in PBS, and stained with Alexa Fluor 488- phalloidin. Images were acquired on an Olympus IX70 microscope, equipped with an Olympus XM10 digital camera and cellSens software (Olympus, Japan).

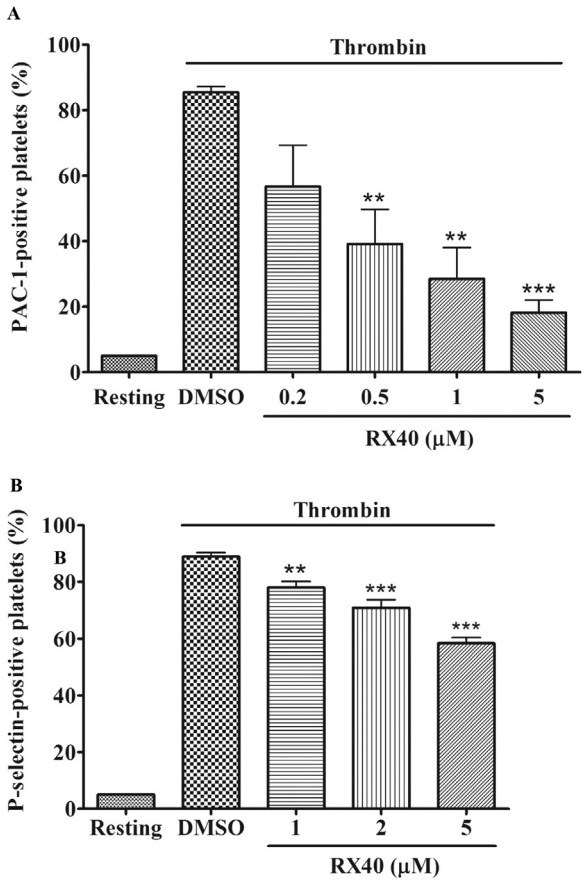

Fig. 2. HPW-RX40 inhibits GPIIb/IIIa activation and P-selectin expression. Washed human platelets were incubated with DMSO or various concentrations of HPW-RX40 for 3 min and then treated with or without thrombin (0.1 U mL^{-1}) in the presence of FITC-conjugated PAC-1 (A) or FITC-conjugated P-selectin Ab (B) for 15 min at room temperature. The samples were fixed with 1% (w/v) paraformaldehyde. The binding of FITC-conjugated antibodies was analyzed by flow cytometry. Results are presented as mean ± SEM (n = 3). $^{**}p < 0.01$, $^{***}p < 0.001$ as compared with the control group.

2.9. Synthesis of the PDI substrate, dieosin glutathione disulfide (Di-E-GSSG)

Di-E-GSSG was synthesized according to the methods described previously [26,27]. Briefly, Solid GSSG (4 mg) and eosin isothiocyanate (14 mg) were mixed in 10 mL of 0.1 M potassium phosphate buffer (pH 9.0) and incubated at 37 °C overnight. Precipitation using acetonitrile containing 0.1% (w/v) trifluoroacetic acid was carried out with a 1 : 3 vol ratio of Di-E-GSSG/acetonitrile (v/v). After precipitation, the pellet composed of Di-E-GSSG formed, and the supernatant was discarded. The pellet was vacuum drained and dissolved in 100 mM potassium phosphate buffer (pH 7.5) to a concentration of 150 μM and stored at −20 °C.

2.10. Di-E-GSSG assay for measuring the activity of recombinant PDI and surface PDI in platelets

In Di-E-GSSG assay, the reduction activity of PDI was measured by the fluorescent eosin-coupled glutathione (EGSH) reduced from the non-fluorescent Di-E-GSSG. Recombinant PDI family proteins (20 or 100 nM) were incubated with HPW-RX40 in the presence of Di-E-GSSG (150 nM). The reaction was started by adding DTT (5 μM of final concentration), and the fluorescence of EGSH (Ex 508 nm/Em 560 nm) was recorded by a microplate fluorescence reader (Synergy HT, BioTek, Winooski, VT, USA). The PDI activity was presented as the increase in fluorescence (in relative fluorescence units). For determination of platelets surface PDI activity, platelets (8×10^7 mL^{-1}) were pretreated with HPW-RX40 or phenylarsine oxide (a PDI inhibitor) for 3 min at 37 °C before addition of Di-E-GSSG (150 nM). As mentioned above, the reaction was started by adding DTT and continuously recorded for 60 min at 37 °C.

2.11. Molecular docking study

The molecular docking study was performed on an Asus personal computer with Intel(R) Core(TM) 2 Quad 2.4 GHz processor, running Windows 7 using ChemBioOffice 2008 [28] and Discovery Studio 3.0 (DS 3.0). The crystal structure was downloaded from the Protein Data Bank (http://www.rcsb.org/pdb/index.html; PDB code: 4EKZ). HPW-RX40 was built with ChemBio3D of ChemBioOffice and minimized using the mmff94 forcefield until a RMSD gradient of 0.05 kcal mol^{-1} $Å^{-1}$ was reached. Partial charges were automatically calculated and the structure was saved as a mol file. Simulations were carried out using the DS LigandFit docking module. The docking space covering CGHC of PDI was expanded, used to construct the binding site. Two possible docked poses of HPW-RX40 were illustrated in the UCSF Chimera 1.10 graphics environment [29].

2.12. Cell culture and evaluation of cell viability

The human breast adenocarcinoma cell line MDA-MB-231, human lung adenocarcinoma cell line A549, and the human umbilical endothelial cell line EA.hy926 were obtained from the American Tissue Culture Collection (ATCC, Manassas, VA, USA). The cells were cultured and maintained as previously described [18]. Cells were seeded into a 96-well plate and treated with the various concentrations of drugs. After 24 h, 100 μL of MTT solution (0.5 mg mL^{-1}) was added to each well. Cells were then incubated at 37 °C for 3 h. The MTT crystals were solubilized with 100 μL of DMSO, and the absorbance was read at 550 nm.

2.13. Western blot analysis

After treatment, cells were washed with ice-cold PBS and then lysed on ice for 30 min with TritonX-100 lysis buffer (pH 7.5, 150 mM NaCl, 50 mM HEPES, 1 mM EGTA, 1.5 mM $MgCl_2$, 1% (v/v) Triton X-100, 10% (v/v) glycerol, protease inhibitors, phosphatase inhibitors). Lysates were centrifuged at 13,000 rpm for 10 min and the supernatant was collected. The protein concentration of the supernatant was determined using the Bradford protein assay (Bio-Rad, Hercules, California). Equal amounts of proteins were loaded and separated by 10% SDS PAGE, and transferred to nitrocellulose membranes. Membranes were incubated overnight at 4 °C with specific primary antibodies. After 1 h incubation with appropriate horseradish peroxidase conjugated secondary antibodies, the immunoreactive bands of target proteins were detected using the enhanced chemiluminescence (ECL) reagent (Millipore, Billerica, MA, USA).

2.14. Statistics

Results are expressed as the mean ± standard error of the mean (SEM), and statistical significance was calculated by one way analysis of variance or two way analysis of variance (ANOVA). $p < 0.05$ was considered statistically significant.

3. Results

3.1. HPW-RX40 inhibits human platelet aggregation induced by various receptor agonists

In human platelet suspension, HPW-RX40 (0.2–5 μM) concentration-dependently inhibited platelet aggregation induced by thrombin (0.05 U mL^{-1}), collagen (5 μg mL^{-1}) and the thromboxane A_2 analogue

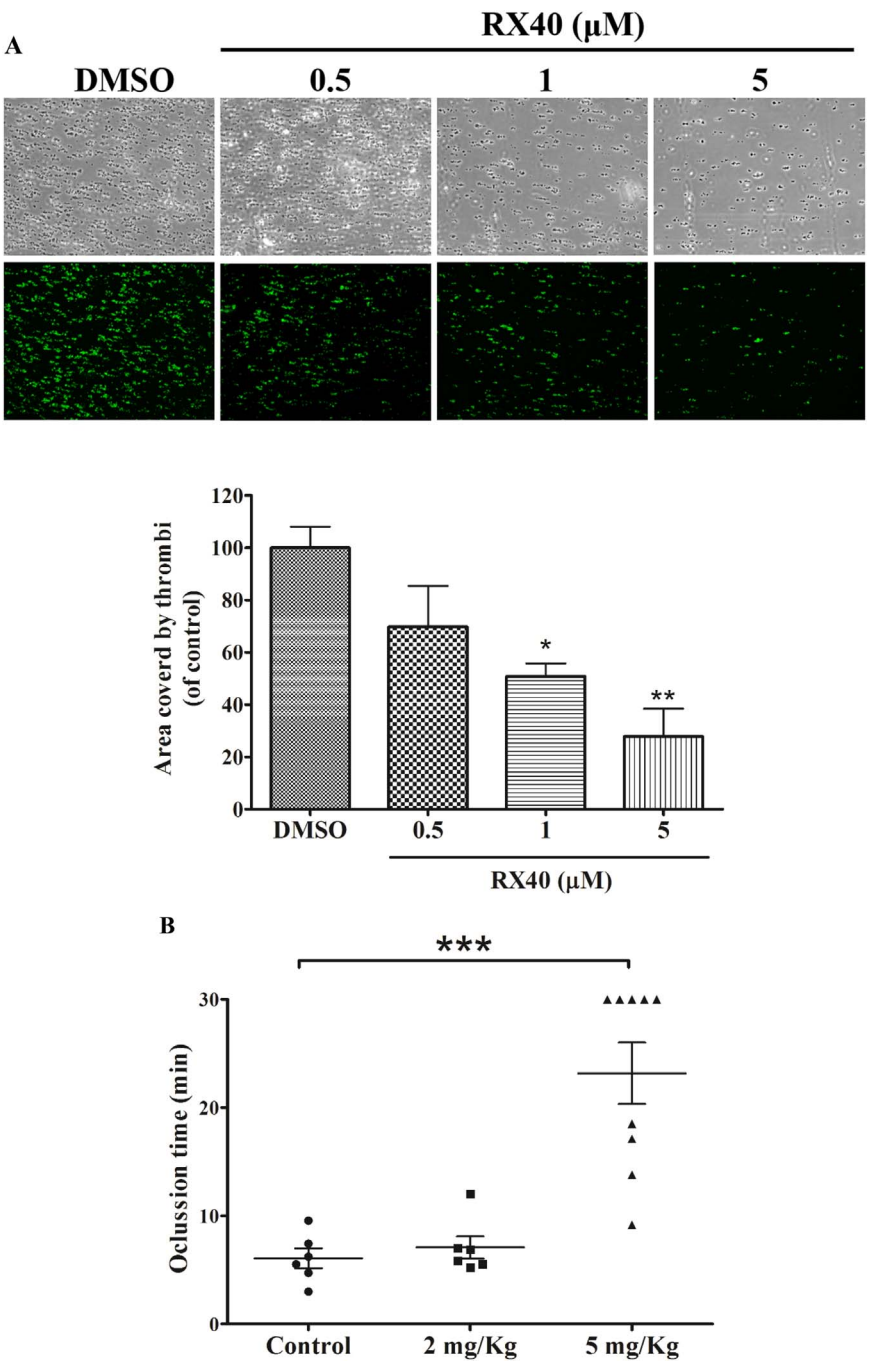

Fig. 3. HPW-RX40 inhibits thrombus formation *in vitro* and *in vivo*. (A) Platelets in citrated whole blood were labeled with $DiOC_6(3)$ 2 μM for 10 min at 37 °C in the absence or presence of HPW-RX40. Labeled blood was perfused through the flow chamber (μ-Slide VI 0.1) for 2 min at a wall shear rate of 1500 S^{-1} (15 dyn cm^{2-1}), and followed by washing with PBS buffer to remove non-adherent cells. Fluorescent (lower panels) and transmitted light (upper panels) images of platelet thrombi were taken using a fluorescence microscope. Area covered by platelet thrombi (fluorescent) was quantified. Values are presented as means ± SEM (n = 3). $*p < 0.05$, $**p < 0.01$ as compared with the DMSO control. (B) HPW-RX40 (2 or 5 mg kg^{-1}; dissolved in normal saline containing 20% PEG400 and 20% Tween80) or vehicle control was administrated by intraperitoneal injection 30 min prior to $FeCl_3$-induced injury of carotid artery. The carotid artery was treated with 10% (w/v) $FeCl_3$ for 3 min, and the blood velocity in the carotid artery was monitored by the small animal Doppler probe for 30 min. Data points represent time to occlusion, and values were expressed as mean ± SEM, n = 6–9 per group. $***p < 0.001$ as compared with the control group.

U46619 (2 μM) with IC_{50} values of 1.56 ± 0.1, 0.65 ± 0.2, and 1.24 ± 0.1 μM, respectively (Fig. 1). Because HPW-RX40 inhibited platelet aggregation caused by different receptor agonists in a similar concentration range, this led to suggest that HPW-RX40 might affect the intersections between different signaling pathways activated by various agonists.

3.2. HPW-RX40 inhibits platelet GPIIb/IIIa activation and P-selectin expression

The conformational change of GPIIb/IIIa and sequential activation is the common and final pathway involved in all stimuli-induced platelet aggregation. In the present study, platelet GPIIb/IIIa activation was determined by using flow cytometry and FITC-labeled PAC-1 antibody which specifically binds to activated GPIIb/IIIa. The percentage of PAC-1-bound platelets was increased from resting levels of 5% to 85% in thrombin-stimulated platelets. HPW-RX40 (0.2–5 μM) reduced PAC-1-bound platelets in response to thrombin in a concentration-dependent manner, indicating that HPW-RX40 is able to prevent GPIIb/IIIa activation (Fig. 2A).

In addition, we tested the effect of HPW-RX40 on platelet secretion by using FITC-labeled anti-P-selectin antibody. P-selectin, a component in platelet α-granule, is released and expressed on platelet surface membrane, thereby serving a marker of platelet secretion. In the same experimental condition as measuring PAC-1-bound platelets, HPW-RX40 also inhibited thrombin-induced surface P-selectin expression on platelets (Fig. 2B), but the inhibitory effect is less potent than that observed in the assay of GPIIb/IIIa activation.

3.3. HPW-RX40 reduces thrombus formation in vitro and in vivo

According to the inhibitory effect of HPW-RX40 on platelet

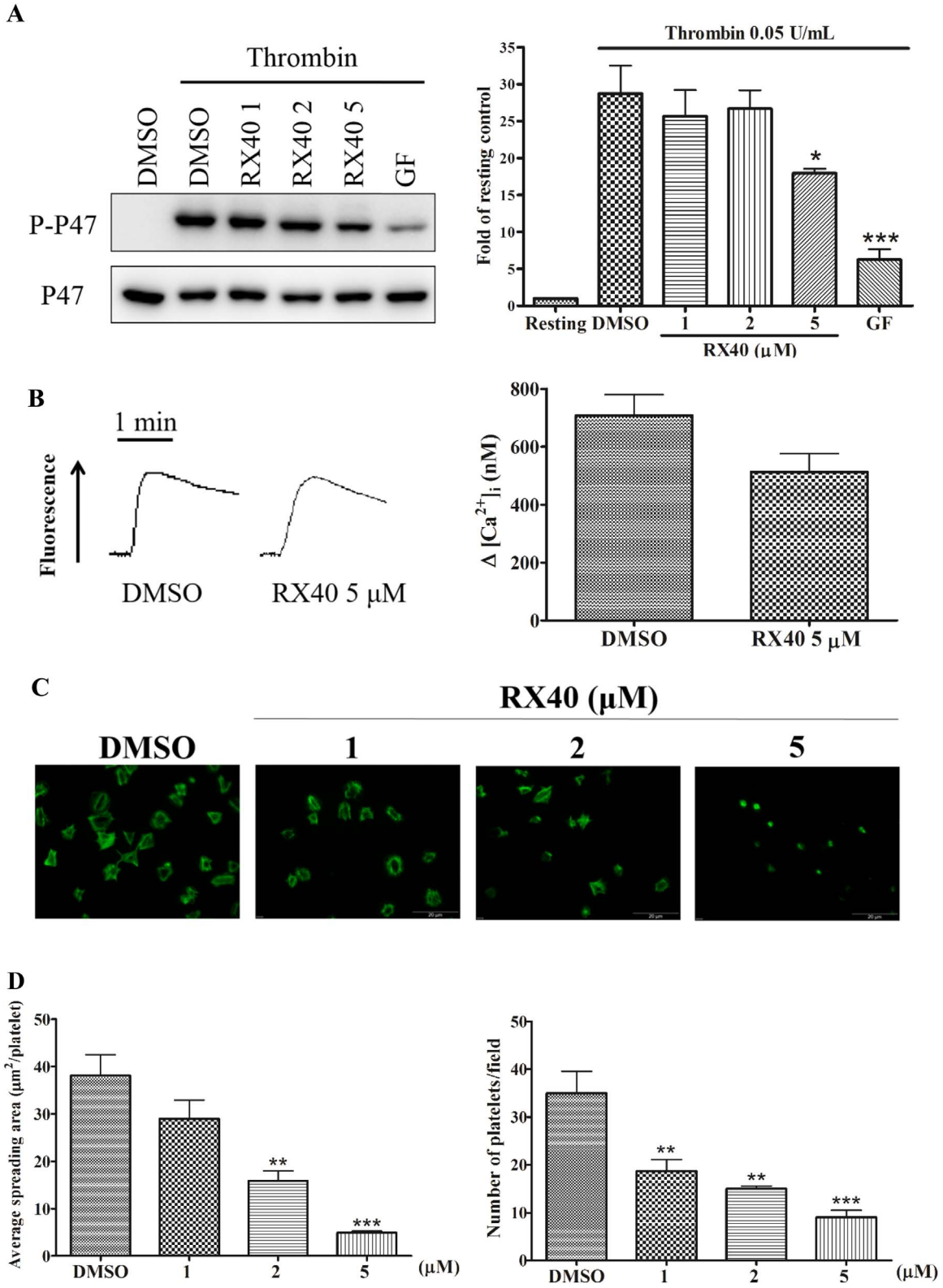

Fig. 4. Effects of HPW-RX40 on "inside-out" and "outside-in" signaling. (A) Washed platelets were incubated with HPW-RX40 (5 μM) or GF-109203X (GF, 5 μM) at 37 °C for 3 min. After then, platelets were treated with or without 0.05 U mL^{-1} thrombin for 1 min. Western blot analysis was performed on whole platelet lysates using phospho-PKC substrate antibody and anti-P47 antibody. Blots were quantified and represented as shown (data are means ± SEM, n = 3). (B) Fura-2-loaded human platelets were incubated with DMSO or HPW-RX40 (5 μM) at 37 °C for 3 min in the presence of 1 mM extracellular Ca^{2+}, then thrombin (0.05 U mL^{-1}) was added to trigger the increase of $[Ca^{2+}]_i$. (C) Washed human platelets were allowed to adhere to fibrinogen-coated surfaces in the presence of DMSO or HPW-RX40 for 1 h. Cells were fixed and stained for F-actin using phalloidin–Alexa Fluor®488, and observed under a fluorescence microscope. Area covered by platelets was quantified. Values are presented as means ± SEM (n = 3). ***$p < 0.001$ as compared with the DMSO control (n = 3).

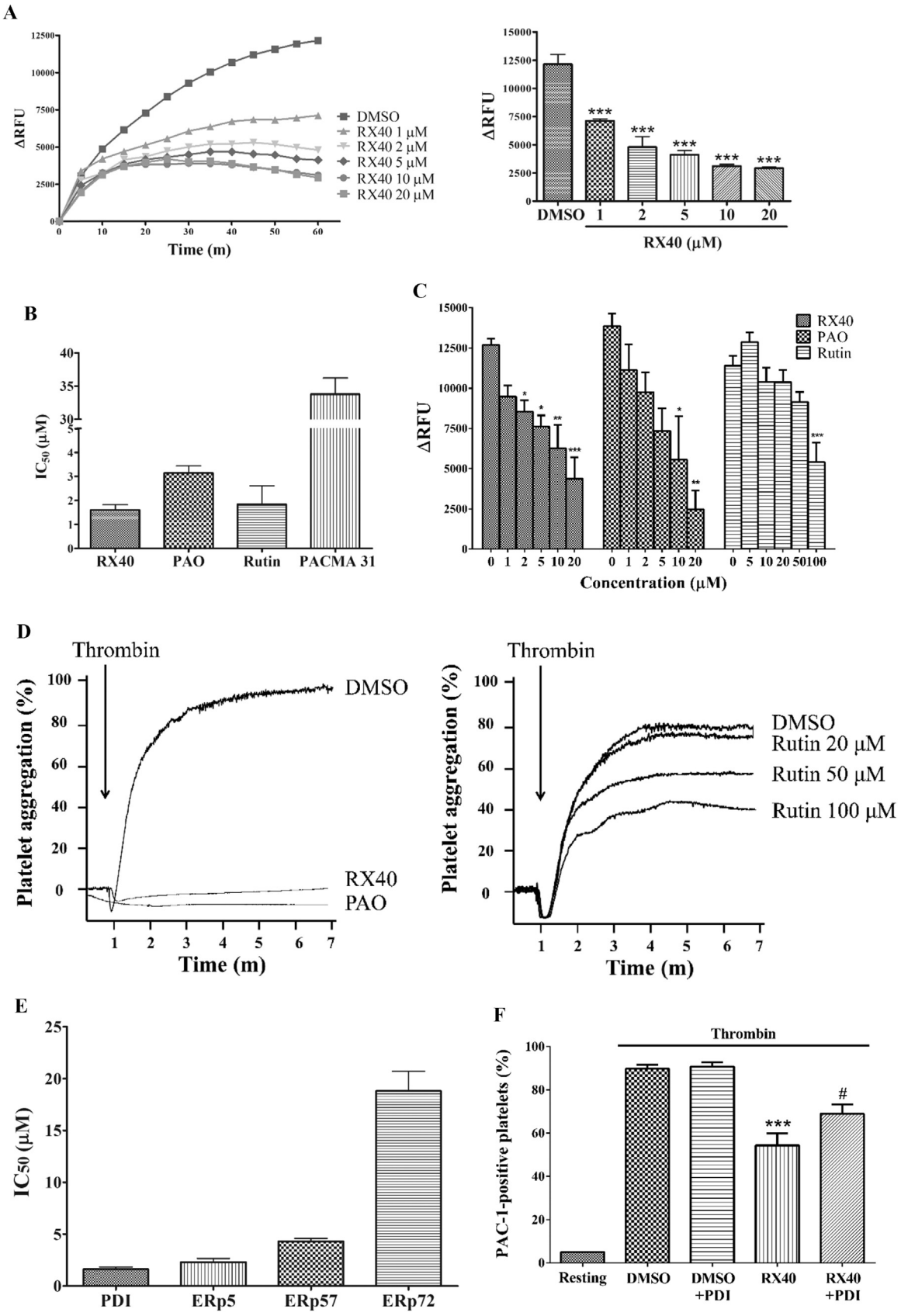

(caption on next page)

Fig. 5. HPW-RX40 inhibits recombinant PDI and reduces the activity of platelet surface PDIs. (A) Recombinant PDI (20 nM) was incubated with Di-E-GSSG (150 nM) and various concentrations of HPW-RX40 for 3 min, and reaction was started by adding DTT (5 μM). PDI activity was measured by monitoring the change in fluorescence (Ex 508 nm/Em 560 nm) for 60 min (B) Inhibitory effects of HPW-RX40, phenyl arsenoxide (PAO), rutin, or PACMA31 on human recombinant PDI were measured by Di-E-GSSG assay. Result was presented as IC_{50} values. (C) Washed human platelets were incubated with HPW-RX40, PAO, or rutin for 3 min, then platelet surface PDI activity was measured by Di-E-GSSG assay. (D) Washed human platelets were incubated with DMSO, PAO, or rutin at 37 °C for 3 min, then thrombin (0.05 U mL^{-1}) was added to trigger platelet aggregation. (E) IC_{50} values of HPW-RX40 for human recombinant PDI, ERp5, ERp57, and ERp72. (F) Washed human platelets were incubated with human recombinant PDI (0.5 μM) for 7 min before adding DMSO or HPW-RX40 (0.5 μM) and then treated with or without thrombin (0.1 U mL^{-1}). The binding of PAC-1 was determined by flow cytometry. Results are presented as mean ± SEM (n = 3). *** $p < 0.001$ as compared with the control group. #$p < 0.05$ as compared to the HPW-RX40 alone group.

aggregation in washed platelet suspension, we further investigated if it could prevent thrombus formation *in vitro* and *in vivo*. The in vitro thrombotic model was conducted using a collagen-coated chamber with flowing whole blood to mimic arterial thrombosis. The progression of platelet adhesion and thrombus formation on a collagen surface in whole blood under arterial flow conditions (at a shear rate of 1500 S^{-1}) was observed in the control group, whereas treatment with HPW-RX40 (1 and 5 μM) significantly reduced platelet aggregates/thrombi (Fig. 3A).

To further test the antithrombotic effect of HPW-RX40 *in vivo*, a murine model of $FeCl_3$-induced carotid artery thrombosis was used. In the control group, the injured carotid artery was occluded by thrombus approximately in 6 min. Treatment of mice with HPW-RX40 significantly prolonged the occlusion time at a dose of 5 mg kg^{-1} compared with the control group (Fig. 3B).

3.4. Effects of HPW-RX40 on signaling pathways involved in platelet activation

Upon platelet stimulation by various agonists through their receptors, PLC represents a central and common signaling pathway involved in GPIIb/IIIa activation [30]. Therefore, the effects of HPW-RX40 on the main downstream signaling events of PLC, *i.e.* PKC activation and intracellular calcium mobilization, were investigated. HPW-RX40 displayed no effect on thrombin-induced phosphorylation of $P47_{phox}$ (a main substrate of PKC in platelets), except at a high concentration (37.5% inhibition at 5 μM) (Fig. 4A). In addition, HPW-RX40 had little effect on thrombin-induced intracellular Ca^{2+} mobilization (Fig. 4B).

We next investigated the effect of HPW-RX40 on platelet adhesion and spreading on immobilized fibrinogen, this process is known to be mediated by GPIIb/IIIa-mediated outside-in signaling [31]. In the presence of HPW-RX40 (1–5 μM), platelet adhesion and spreading were reduced by up to 74.3% and 87.2%, respectively (Fig. 4C), suggesting that GPIIb/IIIa-mediated outside-in signaling was markedly prevented by this compound.

3.5. HPW-RX40 inhibits PDI activity

Given that PDI plays a critical role in both GPIIb/IIIa activation and GPIIb/IIIa-mediated outside-in signaling, we wanted to investigate if the antiplatelet effect of HPW-RX40 is due to PDI inhibition. In the present study, the reductase activity of PDI was determined using a synthetic substrate Di-E-GSSG which can be converted to a florescent product EGSH by PDI. The advantages of Di-E-GSSG assay are that it is more sensitive than insulin turbidity assay and suitable for cellular systems [27]. HPW-RX40 concentration-dependently inhibited the activity of human recombinant PDI with an IC_{50} value of 1.45 μM (Fig. 5A).

Comparing with the putative PDI inhibitors, HPW-RX40 was equally potent as rutin in inhibiting recombinant PDI, and better than PAO and PACMA 31 (Fig. 5B). In human platelets, HPW-RX40 and PAO showed similar potency in inhibiting surface PDI, whereas rutin was much less potent in this system (Fig. 5C). In parallel with their inhibitory effects on platelet surface PDI, rutin was weaker than either HPW-RX40 or PAO in suppressing thrombin-induced platelet aggregation (Fig. 5D).

We next examined the selectivity of HPW-RX40 against a panel of purified recombinant PDI family enzymes, including ERp5, ERp57, and ERp72. HPW-RX40 inhibited these PDI family enzymes with different potency, the rank order of IC_{50} values was: PDI (1.45 μM) < ERp5 (2.6 μM) < ERp57 (4.3 μM) « ERp72 (18.8 μM) (Fig. 5E).

We further investigated if exogenously added PDI prevents HPW-RX40's antiplatelet effects. HPW-RX40 inhibition of GPIIb/IIIa was partially prevented by an equal concentration of recombinant PDI (Fig. 5F), suggesting that platelet surface PDI is one of the targets of HPW-RX40 and that PDI inhibition contributes to the compound's antiplatelet effects.

3.6. Reversible PDI inhibition contributes to HPW-RX40's antiplatelet effects

The reversibility of HPW-RX40 inhibition of PDI was studied using the dilution method. Recombinant PDI at 2 μM (a 100-fold the concentration used in the standard assay) was incubated with HPW-RX40 (10 μM) for 30 min, then the sample was diluted 100 times with assay buffer and subjected to the Di-E-GSSG assay. The reductase activity of HPW-RX40-treated PDI was totally recovered by 100-fold dilution, indicating that the inhibition of PDI by this compound is reversible (Fig. 6A). Similar reversibility of HPW-RX40 could also be observed in platelet aggregation assay (Fig. 6B).

Many reported PDI inhibitors, including PAO, suppress PDI activity by covalent binding to cysteine sulfhydryl groups in the active site of PDI. In the co-presence of excess reduced thiols, such as glutathione (γ-Glu-Cys-Gly, GSH), the most abundant cellular thiol, the potency of sulfhydryl-reacting PDI inhibitors can be attenuated. In the presence of 2 mM GSH, the inhibitory action of PAO on platelet aggregation was largely prevented, while HPW-RX40's action was not affected (Fig. 6C).

In order to understand how HPW-RX40 interacts with PDI, a molecular docking study was performed. HPW-RX40 was docked at the active site of PDI using Protein Data Bank structure, ID code 4EKZ, and it could adopt two possible configurations: one forms a hydrogen bond between the terminal oxygen atom of the nitro moiety of HPW-RX40 and the hydrogen atom of Gly398 backbone nitrogen (1.978 Å), and the other forms an additional hydrogen bond between the bridge oxygen atom of the ether linkage of HPW-RX40 and the hydrogen atom of Trp396 sidechain indole nitrogen (1.858 Å and 2.142 Å) (Fig. 6D).

3.7. Effects of HPW-RX40 on cell viability and ER stress

PDIs in ER are responsible for the protein folding process. Inhibition of PDIs is able to induce unfolded protein response and ER stress, prolonged activation of the response can lead to cell death [32]. In cancer cells, even higher levels of PDI are needed to cope with increased protein synthesis and accompanied elevation of ER stress. Therefore, some PDI inhibitors are developed as anticancer agents [33]. We would like to examine if HPW-RX40 interferes with ER function and exhibits cytotoxicity. Since platelets have limited ER function, two human cancer cell lines (A549 and MDA-MB-231) and a human umbilical endothelial cell line (EA.hy926) were used in our study. In cytotoxicity assay, HPW-RX40 showed no effect on cell viability of these cell lines at the concentrations that inhibit platelet aggregation. These results were consistent with our previous study in which HPW-RX40 was non-toxic to several human breast cancer cell lines in monolayer culture conditions [34]. In contrast, PAO caused significant cytotoxicity

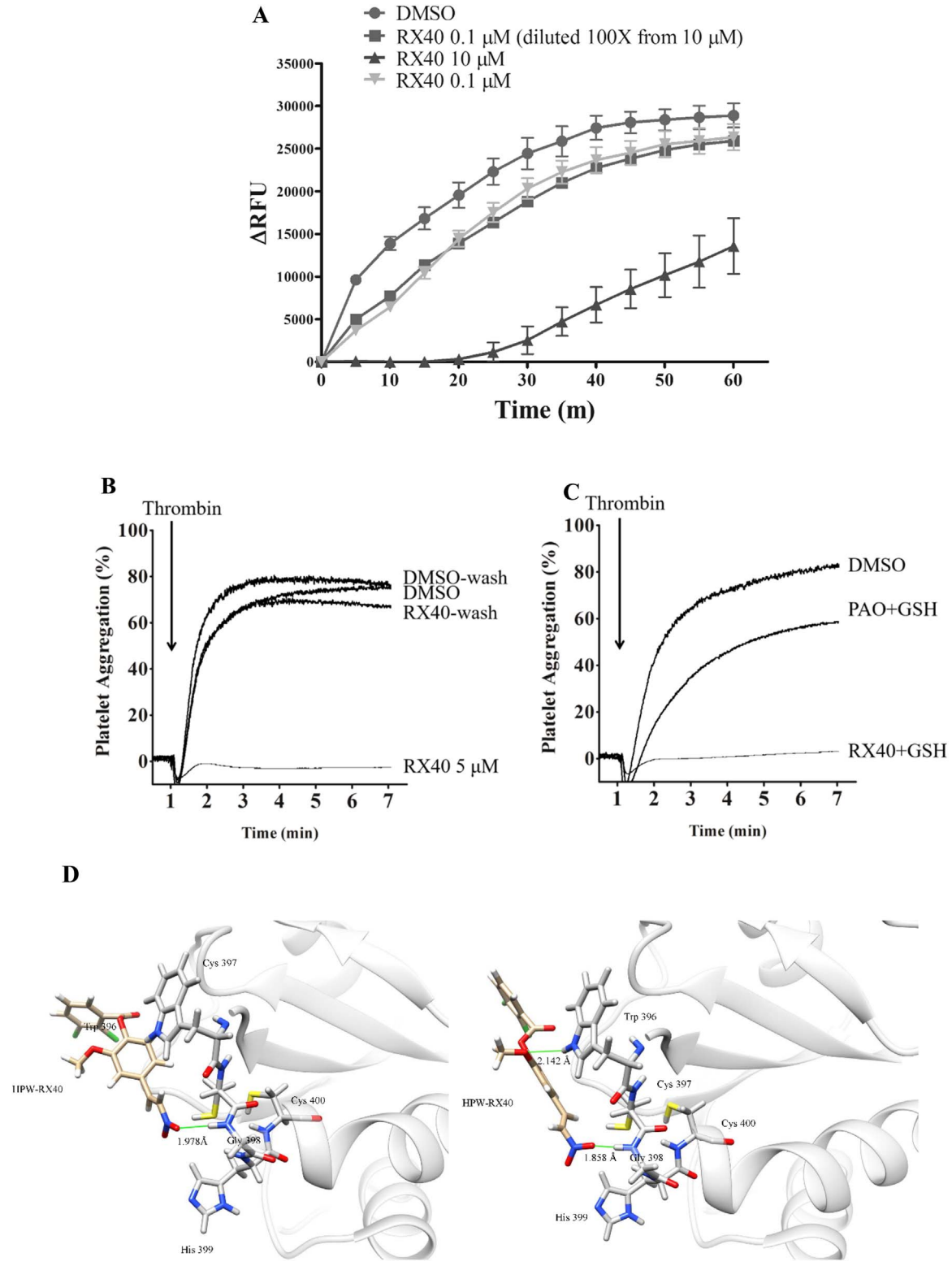

Fig. 6. Reversibility of HPW-RX40 inhibition of PDI and platelet aggregation. (A) Recombinant PDI (2 μM) was incubated with HPW-RX40 (10 μM) for 30 min and subsequently diluted 100-fold in the assay buffer (■). The activity of PDI was compared to samples containing 20 nM PDI in the absence (●) or presence of 0.1 μM (▼) or 10 μM (▲) RX40. (B) Washed human platelets were incubated with DMSO or HPW-RX40 (5 μM) at 37 °C for 3 min. After washing once with Tyrode's solution, platelets were stimulated with thrombin (0.05 U mL^{-1}) to trigger platelet aggregation. (C) Washed human platelets were pretreated with HPW-RX40 (5 μM) or PAO (5 μM) for 3 min in the absence or presence of GSH (2 mM), and stimulated with thrombin (0.05 U mL^{-1}) to induce platelet aggregation. (D) Docking simulations show that HPW-RX40 interacts with the active site of PDI in two possible configurations. Left panel: HPW-RX40 (mostly in tan) forms a hydrogen bond (in green) with Gly398. Right panel: HPW-RX40 forms an additional hydrogen bond with Trp396. (For interpretation of the references to color in this figure legend, the reader is referred to the web version of this article).

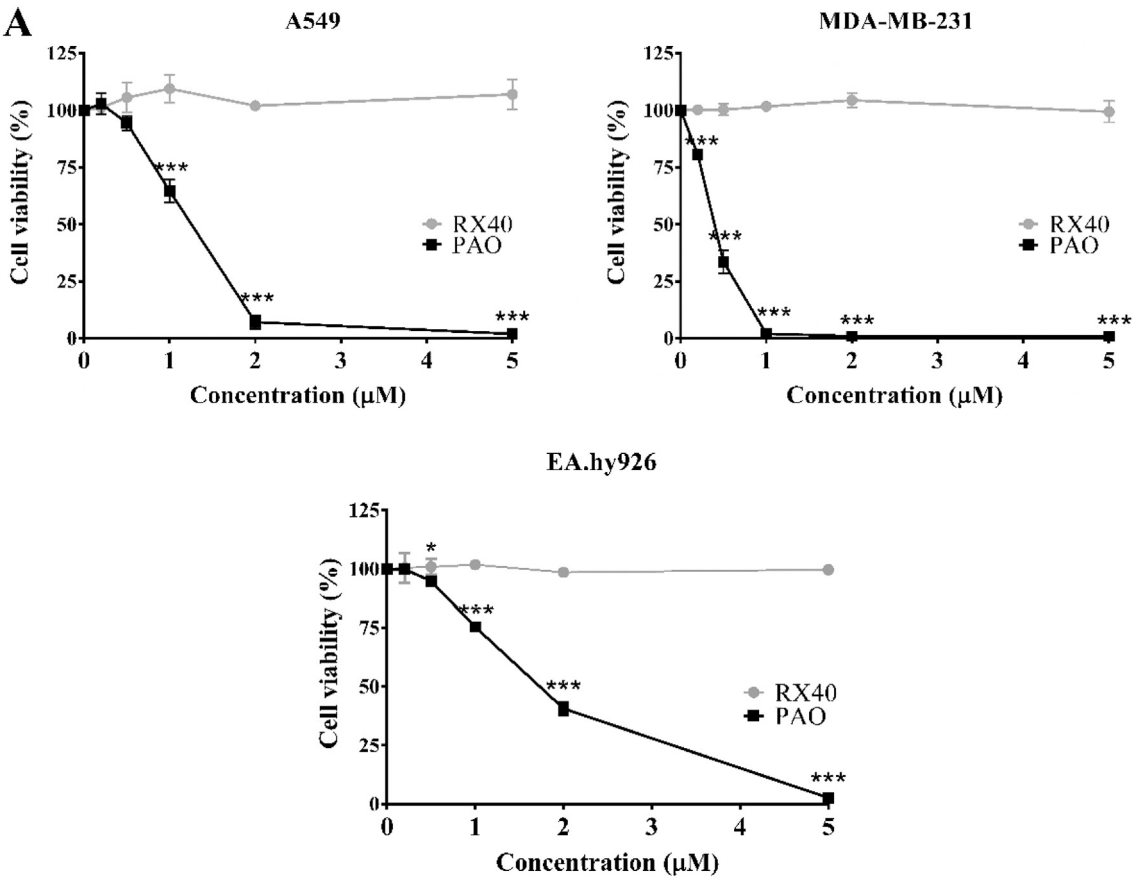

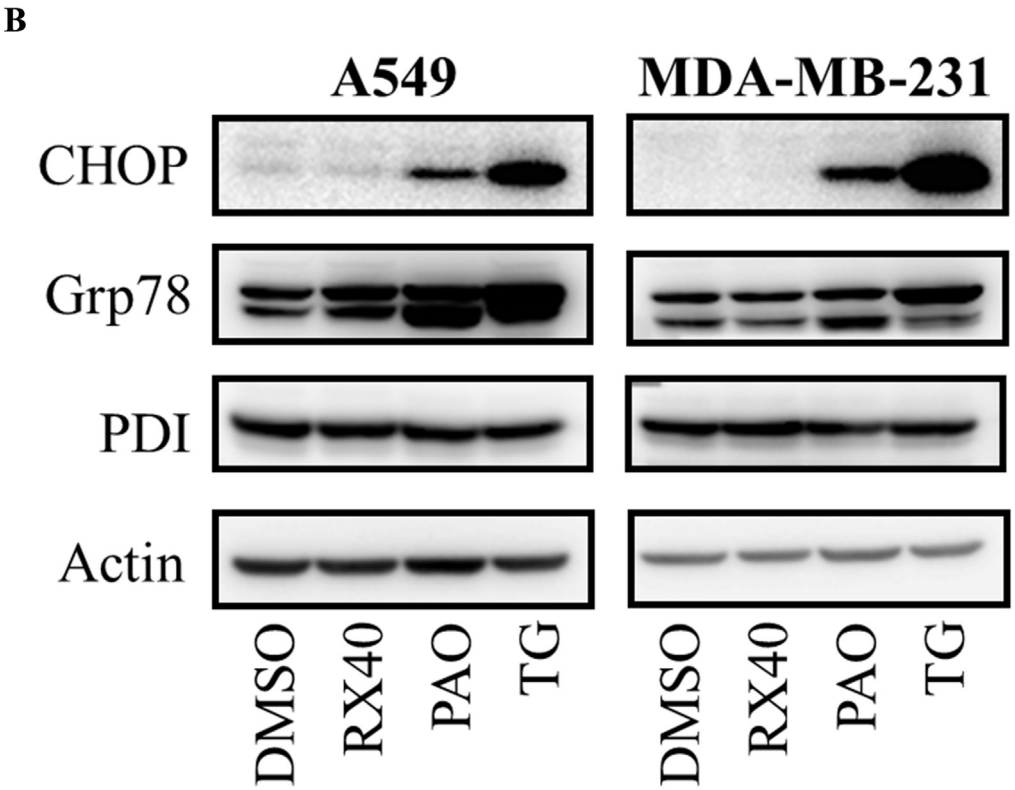

Fig. 7. Effects of HPW-RX40 and PAO on cell viability and ER stress markers in human cell lines. (A) Human lung cancer A549 cells, breast cancer MDA-MB-231 cells, and human umbilical vein EA. hy926 cells were treated with DMSO, HPW-RX40 (0.2–5 μM), or PAO (0.2–5 μM) for 24 h, then the cell viability was measured by MTT assay (n = 3). $*p < 0.05$, $***p < 0.001$ as compared with the PAO positive control. (B) A549 and MDA-MB-231 cells were incubated with DMSO, HPW-RX40 (5 μM), PAO (1 μM for MDA-MB231 and 2 μM for A549), or thapsigargin (TG, 100 nM) for 24 h. The cells were harvested and whole-cell lysates were subjected to immunoblot with antibodies against the indicated proteins. Results are representative of three independent experiments.

even at low concentrations (Fig. 7A).

Next, the protein levels of CHOP and GRP78, which are the downstream components of ER stress [35], were determined by Western blotting. HPW-RX40 (5 μM) had little or no effects on CHOP/GRP78 expression in A549 and MDA-MB-231 cells. In contrast, both PAO (2 and 5 μM) and the ER stress inducer thapsigargin significantly induced CHOP/GRP78 expression in cancer cells (Fig. 7B).

4. Discussion

GPIIb/IIIa is the major integrin present in platelets. Like other integrins, GPIIb/IIIa contains a great number of cysteine residues and several disulfide bonds in both α and β subunit, especially in the EGF domains of β subunit [36,37]. Reduction and/or rearrangement of disulfide bonds in EGF dominant has been reported to promote the ligand-binding affinity of GPIIb/IIIa [38,39]. PDI on platelet surfaces is considered to play an important role in catalysis of the thiol/disulfide exchange and involved in GPIIb/IIIa activation [40]. Besides PDI, other members of the PDI family, including ERp5, ERp57, ERp72, ERp44, and TMX3, also exist in platelets [41]. Like PDI inhibition, blockade of either ERp5 or ERp57 has been demonstrated to suppress GPIIb/IIIa activation, platelet aggregation, secretion, and *in vivo* thrombus formation [23,42–44], suggesting that the different PDIs are necessary for optimal platelet aggregation.

In the present study, we show that HPW-RX40 potently inhibited the activity of PDI, ERp5, and ERp57 (IC_{50}: 1.5–4.3 μM), but was less potent in inhibiting ERp72. The PDIs-inhibiting effect correlated well with HPW-RX40's actions on GPIIb/IIIa activation and platelet aggregation. In addition, HPW-RX40 had little effect on the “inside-out” signaling, *i.e.* PKC activation and intracellular Ca^{2+} mobilization, while significantly prevented the “outside-in” signaling as evident with a decrease in platelet adhesion and spreading on fibrinogen, all of which fit the characteristics of PDI inhibition in platelets. Furthermore, HPW-RX40 inhibition of GPIIb/IIIa was partially rescued by exogenous PDI, indicating that the antiplatelet effect of HPW-RX40 is due to, at least in part, suppression of platelet surface PDI.

The structure of PDI is composed by two catalytic domains (a and a′) and two substrate binding domains (b and b′) [45,46]. The catalytic domains contain Cys-XX-Cys active site motifs responsible for thiol/disulfide exchange [40]. Many chemical compounds, such as bacitracin, arsenics or sulfhydryl reagents, have been reported to inhibit PDI by forming covalent bonds with the cysteine residues in the active sites, but they usually lack either potency or selectivity [6,47–49]. Newly identified PDI inhibitors, such as PACMA31, and CCF642, are more selective toward PDI, but they also irreversibly bind to the active site cysteine residues and exhibit potent cytotoxicity [50–52]. This property may be of benefit for treatment of cancer effectively; however, it is apparently not suitable for treating non-malignant diseases, such as cardiovascular diseases. We show here that HPW-RX40 inhibited PDI by a distinct mechanism different from that of irreversible PDI inhibitor. The inhibitory effects of HPW-RX40 on PDI activity and platelet aggregation were reversible. In addition, there are two lines of evidence suggesting that the action of HPW-RX40 is not *via* a thiol-dependent mechanism. First, exogenous administration of reduced glutathione prevented the antiplatelet effect of PAO but not that of HPW-RX40. Second, the molecular docking study did not support that HPW-RX40 forms covalent bonds with Cys397 or Cys400 in the active sites. Instead, HPW-RX40 tends to form hydrogen bonds with adjacent Gly398 or Trp396. Of note, the interaction between Trp396 in the active site and Arg300 in the b′ domain involves in the redox-dependent conformational change of PDI [53,54]. Further studies are needed to see if HPW-RX40 affects this interaction.

Recently, a natural flavonoid, rutin (quercetin-3-O-rutinoside), was found to reversibly inhibit PDI and to exhibit *in vivo* and *in vitro* antiplatelet activities; one of its analogs has entered the clinical trials [55]. In the present study, we show that rutin potently inhibited purified recombinant PDI, but it required much higher concentrations to inhibit platelet surface PDI activity and platelet aggregation. One possibility is that rutin is a selective inhibitor towards PDI and the other PDI family enzymes (ERp57 and ERp5) in platelets may compensate for the inhibition. Another possibility may come from the conformational difference between soluble and membrane-bound forms of PDI. On platelet surfaces, PDI binds to β subunit of GPIIb/IIIa with its substrate binding (b and b′) domains, but not the catalytic domains [56,57]. Because rutin acts as an allosteric inhibitor of PDI by binding at a site in b′ domain [58], it might not inhibit membrane-bound PDI whose substrate binding domains are hindered by GPIIb/IIIa. In contrast, the docking assay revealed that HPW-RX40 binds to the catalytic a′ domain of PDI, this may explain its inhibitory effects on both the soluble and membrane-bounded forms of PDI.

In summary, our results indicate that HPW-RX40 is a reversible inhibitor of platelet surface PDI, this effect is accompanied by suppression of platelet aggregation and thrombus formation. Furthermore, HPW-RX40 has no significant influence on ER stress and is non-toxic to certain human cancer cells. These features make this compound a potential candidate for development of new antiplatelet drugs for treating arterial thrombosis.

Conflicts of interest

The authors have no conflicts of interest.

Acknowledgment

This work was supported by grants from the Ministry of Science and Technology, Taiwan (MOST 103-2320-B-037-013-MY3).

References

[1] F.R. Laurindo, L.A. Pescatore, C. Fernandes Dde, Protein disulfide isomerase in redox cell signaling and homeostasis, Free Radic. Biol. Med. 52 (2012) 1954–1969.
[2] L. Wang, X. Wang, C.C. Wang, Protein disulfide-isomerase, a folding catalyst and a redox-regulated chaperone, Free Radic. Biol. Med. 83 (2015) 305–313.
[3] J. Cho, Protein disulfide isomerase in thrombosis and vascular inflammation, J. Thromb. Haemost. 11 (2013) 2084–2091.
[4] H. Ali Khan, B. Mutus, Protein disulfide isomerase a multifunctional protein with multiple physiological roles, Front. Chem. 2 (2014) 70.
[5] D.W. Essex, M. Li, Protein disulphide isomerase mediates platelet aggregation and secretion, Br. J. Haematol. 104 (1999) 448–454.
[6] D.W. Essex, M. Li, A. Miller, R.D. Feinman, Protein disulfide isomerase and sulfhydryl-dependent pathways in platelet activation, Biochemistry 40 (2001) 6070–6075.
[7] B.S. Coller, S.J. Shattil, The GPIIb/IIIa (integrin alphaIIbbeta3) odyssey: a technology-driven saga of a receptor with twists, turns, and even a bend, Blood 112 (2008) 3011–3025.
[8] R. Mor-Cohen, Disulfide Bonds as Regulators of Integrin Function in Thrombosis and Hemostasis, Antioxid. Redox Signal. 24 (2016) 16–31.
[9] B. Estevez, K. Kim, M.K. Delaney, A. Stojanovic-Terpo, B. Shen, C. Ruan, J. Cho, Z.M. Ruggeri, X. Du, Signaling-mediated cooperativity between glycoprotein Ib-IX and protease-activated receptors in thrombin-induced platelet activation, Blood 127 (2016) 626–636.
[10] J. Lahav, K. Jurk, O. Hess, M.J. Barnes, R.W. Farndale, J. Luboshitz, B.E. Kehrel, Sustained integrin ligation involves extracellular free sulfhydryls and enzymatically catalyzed disulfide exchange, Blood 100 (2002) 2472–2478.
[11] A. Leader, R. Mor-Cohen, R. Ram, V. Sheptovitsky, U. Seligsohn, N. Rosenberg, J. Lahav, The role of protein disulfide isomerase in the post-ligation phase of beta3 integrin-dependent cell adhesion, Thromb. Res. 136 (2015) 1259–1265.
[12] J. Cho, B.C. Furie, S.R. Coughlin, B. Furie, A critical role for extracellular protein disulfide isomerase during thrombus formation in mice, J. Clin. Investig. 118 (2008) 1123–1131.
[13] K. Kim, E. Hahm, J. Li, L.M. Holbrook, P. Sasikumar, R.G. Stanley, M. Ushio-Fukai, J.M. Gibbins, J. Cho, Platelet protein disulfide isomerase is required for thrombus formation but not for hemostasis in mice, Blood 122 (2013) 1052–1061.
[14] W.Y. Wang, P.W. Hsieh, Y.C. Wu, C.C. Wu, Synthesis and pharmacological evaluation of novel beta-nitrostyrene derivatives as tyrosine kinase inhibitors with potent antiplatelet activity, Biochem. Pharmacol. 74 (2007) 601–611.
[15] W.Y. Wang, Y.C. Wu, C.C. Wu, Prevention of platelet glycoprotein IIb/IIIa activation by 3,4-methylenedioxy-beta-nitrostyrene, a novel tyrosine kinase inhibitor, Mol. Pharmacol. 70 (2006) 1380–1389.
[16] C.K. Wei, F.R. Chang, P.W. Hsieh, C.C. Wu, Inhibition of the interactions between metastatic human breast cancer cells and platelets by beta-nitrostyrene derivatives,

Life Sci. 143 (2015) 147–155.
[17] P.W. Hsieh, Y.T. Chang, W.Y. Chuang, H.C. Shih, S.Z. Chiang, C.C. Wu, The synthesis and biologic evaluation of anti-platelet and cytotoxic beta-nitrostyrenes, Bioorg. Med. Chem. 18 (2010) 7621–7627.
[18] I.H. Chen, F.R. Chang, Y.C. Wu, P.H. Kung, C.C. Wu, 3,4-Methylenedioxy-beta-nitrostyrene inhibits adhesion and migration of human triple-negative breast cancer cells by suppressing beta1 integrin function and surface protein disulfide isomerase, Biochimie 110 (2015) 81–92.
[19] W.Y. Chuang, P.H. Kung, C.Y. Kuo, C.C. Wu, Sulforaphane prevents human platelet aggregation through inhibiting the phosphatidylinositol 3-kinase/Akt pathway, Thromb. Haemost. 109 (2013) 1120–1130.
[20] C.C. Wu, S.Y. Wu, C.Y. Liao, C.M. Teng, Y.C. Wu, S.C. Kuo, The roles and mechanisms of PAR4 and P2Y12/phosphatidylinositol 3-kinase pathway in maintaining thrombin-induced platelet aggregation, Br. J. Pharmacol. 161 (2010) 643–658.
[21] S. Meyer dos Santos, U. Klinkhardt, R. Schneppenheim, S. Harder, Using ImageJ for the quantitative analysis of flow-based adhesion assays in real-time under physiologic flow conditions, Platelets 21 (2010) 60–66.
[22] T. Bonnard, C.E. Hagemeyer, Ferric chloride-induced thrombosis mouse model on carotid artery and mesentery vessel, J. Vis. Exp. e52838 (2015).
[23] Y. Wu, S.S. Ahmad, J. Zhou, L. Wang, M.P. Cully, D.W. Essex, The disulfide isomerase ERp57 mediates platelet aggregation, hemostasis, and thrombosis, Blood 119 (2012) 1737–1746.
[24] C.Y. Liao, C.L. Lee, H.C. Wang, S.S. Liang, P.H. Kung, Y.C. Wu, F.R. Chang, C.C. Wu, CLL2-1, a chemical derivative of orchid 1,4-phenanthrenequinones, inhibits human platelet aggregation through thiol modification of calcium-diacylglycerol guanine nucleotide exchange factor-I (CalDAG-GEFI), Free Radic. Biol. Med. 78 (2015) 101–110.
[25] S. Matsuura, R. Mi, M. Koupenova, A. Eliades, S. Patterson, P. Toselli, J. Thon, J.E. Italiano Jr, P.C. Trackman, N. Papadantonakis, K. Ravid, Lysyl oxidase is associated with increased thrombosis and platelet reactivity, Blood 127 (2016) 1493–1501.
[26] A. Raturi, B. Mutus, Characterization of redox state and reductase activity of protein disulfide isomerase under different redox environments using a sensitive fluorescent assay, Free Radic. Biol. Med. 43 (2007) 62–70.
[27] S.J. Montano, J. Lu, T.N. Gustafsson, A. Holmgren, Activity assays of mammalian thioredoxin and thioredoxin reductase: fluorescent disulfide substrates, mechanisms, and use with tissue samples, Anal. Biochem. 449 (2014) 139–146.
[28] K.R. Cousins, Computer review of ChemDraw Ultra 12.0, J. Am. Chem. Soc. 133 (2011) 8388.
[29] E.F. Pettersen, T.D. Goddard, C.C. Huang, G.S. Couch, D.M. Greenblatt, E.C. Meng, T.E. Ferrin, UCSF Chimera–a visualization system for exploratory research and analysis, J. Comput. Chem. 25 (2004) 1605–1612.
[30] Z. Li, M.K. Delaney, K.A. O'Brien, X. Du, Signaling during platelet adhesion and activation, Arterioscler. Thromb. Vasc. Biol. 30 (2010) 2341–2349.
[31] M. Mehrbod, S. Trisno, M.R. Mofrad, On the activation of integrin alphaIIbbeta3: outside-in and inside-out pathways, Biophys. J. 105 (2013) 1304–1315.
[32] R. Sano, J.C. Reed, ER stress-induced cell death mechanisms, Biochim. Biophys. Acta 1833 (2013) 3460–3470.
[33] S. Xu, S. Sankar, N. Neamati, Protein disulfide isomerase: a promising target for cancer therapy, Drug Discov. Today 19 (2014) 222–240.
[34] I.H. Chen, H.C. Shih, P.W. Hsieh, F.R. Chang, Y.C. Wu, C.C. Wu, HPW-RX40 restores anoikis sensitivity of human breast cancer cells by inhibiting integrin/FAK signaling, Toxicol. Appl. Pharmacol. 289 (2015) 330–340.
[35] C.M. Oslowski, F. Urano, Measuring ER stress and the unfolded protein response using mammalian tissue culture system, Methods Enzymol. 490 (2011) 71–92.
[36] J. Takagi, N. Beglova, P. Yalamanchili, S.C. Blacklow, T.A. Springer, Definition of EGF-like, closely interacting modules that bear activation epitopes in integrin beta subunits, Proc. Natl. Acad. Sci. USA 98 (2001) 11175–11180.
[37] J. Zhu, B.H. Luo, T. Xiao, C. Zhang, N. Nishida, T.A. Springer, Structure of a complete integrin ectodomain in a physiologic resting state and activation and deactivation by applied forces, Mol. Cell 32 (2008) 849–861.
[38] B. Yan, J.W. Smith, A redox site involved in integrin activation, J. Biol. Chem. 275 (2000) 39964–39972.
[39] D.W. Essex, M. Li, Redox modification of platelet glycoproteins, Curr. Drug Targets 7 (2006) 1233–1241.
[40] L. Ellgaard, L.W. Ruddock, The human protein disulphide isomerase family: substrate interactions and functional properties, EMBO Rep. 6 (2005) 28–32.
[41] L.M. Holbrook, N.A. Watkins, A.D. Simmonds, C.I. Jones, W.H. Ouwehand, J.M. Gibbins, Platelets release novel thiol isomerase enzymes which are recruited to the cell surface following activation, Br. J. Haematol. 148 (2010) 627–637.
[42] P.A. Jordan, J.M. Stevens, G.P. Hubbard, N.E. Barrett, T. Sage, K.S. Authi, J.M. Gibbins, A role for the thiol isomerase protein ERP5 in platelet function, Blood 105 (2005) 1500–1507.
[43] F.H. Passam, L. Lin, S. Gopal, J.D. Stopa, L. Bellido-Martin, M. Huang, B.C. Furie, B. Furie, Both platelet- and endothelial cell-derived ERp5 support thrombus formation in a laser-induced mouse model of thrombosis, Blood 125 (2015) 2276–2285.
[44] L.M. Holbrook, P. Sasikumar, R.G. Stanley, A.D. Simmonds, A.B. Bicknell, J.M. Gibbins, The platelet-surface thiol isomerase enzyme ERp57 modulates platelet function, J. Thromb. Haemost. 10 (2012) 278–288.
[45] G. Kozlov, P. Maattanen, D.Y. Thomas, K. Gehring, A structural overview of the PDI family of proteins, FEBS J. 277 (2010) 3924–3936.
[46] A.M. Benham, The protein disulfide isomerase family: key players in health and disease, Antioxid. Redox Signal. 16 (2012) 781–789.
[47] R. Mandel, H.J. Ryser, F. Ghani, M. Wu, D. Peak, Inhibition of a reductive function of the plasma membrane by bacitracin and antibodies against protein disulfide-isomerase, Proc. Natl. Acad. Sci. USA 90 (1993) 4112–4116.
[48] T.A. Bennett, B.S. Edwards, L.A. Sklar, S. Rogelj, Sulfhydryl regulation of L-selectin shedding: phenylarsine oxide promotes activation-independent L-selectin shedding from leukocytes, J. Immunol. 164 (2000) 4120–4129.
[49] M.M. Khan, S. Simizu, M. Kawatani, H. Osada, The potential of protein disulfide isomerase as a therapeutic drug target, Oncol. Res. 19 (2011) 445–453.
[50] R. Banerjee, N.J. Pace, D.R. Brown, E. Weerapana, 1,3,5-Triazine as a modular scaffold for covalent inhibitors with streamlined target identification, J. Am. Chem. Soc. 135 (2013) 2497–2500.
[51] S. Vatolin, J.G. Phillips, B.K. Jha, S. Govindgari, J. Hu, D. Grabowski, Y. Parker, D.J. Lindner, F. Zhong, C.W. Distelhorst, M.R. Smith, C. Cotta, Y. Xu, S. Chilakala, R.R. Kuang, S. Tall, F.J. Reu, Novel protein disulfide isomerase inhibitor with anticancer activity in multiple myeloma, Cancer Res. 76 (2016) 3340–3350.
[52] R. Yamada, X. Cao, A.N. Butkevich, M. Millard, S. Odde, N. Mordwinkin, R. Gundla, E. Zandi, S.G. Louie, N.A. Petasis, N. Neamati, Discovery and preclinical evaluation of a novel class of cytotoxic propynoic acid carbamoyl methyl amides (PACMAs), J. Med. Chem. 54 (2011) 2902–2914.
[53] C. Wang, W. Li, J. Ren, J. Fang, H. Ke, W. Gong, W. Feng, C.C. Wang, Structural insights into the redox-regulated dynamic conformations of human protein disulfide isomerase, Antioxid. Redox Signal. 19 (2013) 36–45.
[54] C. Wang, J. Yu, L. Huo, L. Wang, W. Feng, C.C. Wang, Human protein-disulfide isomerase is a redox-regulated chaperone activated by oxidation of domain a', J. Biol. Chem. 287 (2012) 1139–1149.
[55] R. Jasuja, F.H. Passam, D.R. Kennedy, S.H. Kim, L. van Hessem, L. Lin, S.R. Bowley, S.S. Joshi, J.R. Dilks, B. Furie, B.C. Furie, R. Flaumenhaft, Protein disulfide isomerase inhibitors constitute a new class of antithrombotic agents, J. Clin. Investig. 122 (2012) 2104–2113.
[56] J. Zhou, Y. Wu, L. Wang, L. Rauova, V.M. Hayes, M. Poncz, D.W. Essex, The C-terminal CGHC motif of protein disulfide isomerase supports thrombosis, J. Clin. Investig. 125 (2015) 4391–4406.
[57] J. Cho, D.R. Kennedy, L. Lin, M. Huang, G. Merrill-Skoloff, B.C. Furie, B. Furie, Protein disulfide isomerase capture during thrombus formation in vivo depends on the presence of beta3 integrins, Blood 120 (2012) 647–655.
[58] L. Lin, S. Gopal, A. Sharda, F. Passam, S.R. Bowley, J. Stopa, G. Xue, C. Yuan, B.C. Furie, R. Flaumenhaft, M. Huang, B. Furie, Quercetin-3-rutinoside Inhibits Protein Disulfide Isomerase by Binding to Its b'x Domain, J. Biol. Chem. 290 (2015) 23543–23552.